Single-Particle States of Heavy and Superheavy Nuclei in a Velocity-Dependent Potential *

M. A. K. Lodhi

Department of Physics, Texas Tech University,
Lubbock, Texas 79409

and Institute für Theoretische Kernphysik,
Technische Hochschule Darmstadt, Germany

Single-particle energy calculations have been performed for some closed shell heavy and superheavy nuclei using a form of an effective velocity-dependent nucleon-nucleus potential. Results are compared with other calculations and experimental data wherever available.

The single-particle Hamiltonian for a nucleon bound in a nucleus acconts rather accurately for gross nuclear data of bound as well as scattering states, thus leaving only small many-body forces to produce residual correlations. A phenomenological picture like this allows comprehension of essential facts such as pronounced nuclear shell structure. However, the non-locality character of a single-particle Hamiltonian has been felt rather an essential feature for all types of calculations in studying the heavy and superheavy nuclei [1-9]. The purpose of these calculations is to ingestigate the effect of such a feature on some of the heavy and superheavy closed shell nuclei like ^{208}Pb, $^{284}_{114}X$, and $^{298}_{114}X$. This note reports the results of the single-particle energy calculations for these nuclei in a manner described earlier [1]. We have used the same effective velocity-dependent nucleon-nucleus interaction of the type [1]

$$V(r) = -V_0 f(r) - \frac{\delta \hbar^2}{8 \mu} [\Delta f(r) - 2 \nabla \cdot f(r) \nabla + f(r) \Delta],$$
(1)

where μ is the reduced mass of the system consisting of a nucleon of mass m moving in an average field due to the remaining part of a nucleus of mass number A. The degree of velocity dependence of this potential is characterized by the parameter δ given by

$$\delta = (V_0 \mu b^2) / (2 \hbar^2)$$
(2)

where

$$b^2 = \tfrac{2}{3} \text{ fm}^2 \text{ and } V_0 = 70 \text{ MeV}.$$
(3)

The function $f(r)$ is the real part of the average nuclear potential. Its form is best described as having an approximately uniform interior region and diffuse surface which falls off rapidly within a short distance, say $2-4$ fm, beyond the rms radius. The functional form of $f(r)$ used for these calculation is the well known Woods-Saxon type

$$f(r) = 1/[1 + \exp\{r - R)/d\}],$$
(4)

where

$$R = 1.2 \ A^{1/3} \text{ fm and } d = 0.6485 \text{ fm}.$$

The aim of this work is not to predict exactly the single-particle energy level diagrams for heavy and superheavy nuclei, but only to make some qualitative estimates for these energies using a relatively realistic velocity-dependent potential. Therefore, we have chosen a simple method by approximating the velocity-dependent potential to the well known Morse function. We have ignored the effects due to several terms such as spin-orbit splitting, Coulomb, asymmetry, pairing energy, shell correction, etc. which should be taken care of for finite-nuclei calculations. In fact the spin-orbit splitting particularly for deeply bound states in heavy and superheavy nuclei is reduced to a negligible amount [7]. Since we are concerned with only neutron states presently, the Coulomb term is eliminated by itself. The other perturbation terms should be of little consequence. The overall agreement of the single-particle energies, calculated earlier by using this type of velocity-dependent potential, with the experimental values encouraged us to extend our calculations to the superheavy nuclei in this framework.

Table 1 shows some results of these calculations for single-particle energies for neutrons in ^{208}Pb, $^{284}_{114}X_{170}$, and $^{298}_{114}X_{184}$. The Single-particle assignments near the Fermi surface are in reasonable agreement with other calculations and observed values (only for lead). The low-lying levels are consistent with other calculations. Comparing these single particle energies of the last

Table 1. Single-particle energies for ^{208}Pb, $^{284}_{114}X$, and $^{281}_{194}X$ are given in MeV. The corresponding values in the last column are based on $^{200}_{114}X$.

Nucleus	^{208}Pb		$^{284}_{114}X$	$^{298}_{114}X$		
state	This Work	V—B[12]	This Work	Work This	V—B[12]	MELD-NER [7]
1 s	66.9	44.6	69.5	70.5	44.6	90.0
1 p	63.8	40.7	67.0	68.1	41.6	82.0
1 d	60.0	35.4	63.2	64.2	37.8	72.0
1 f	47.3	29.6	53.4	55.0	32.8	61.3
1 g	38.0	22.6	44.9	46.7	27.4	49.0
1 h	24.2	18.1	33.0	35.2	21.2	37.0
1 i	9.5	6.2	20.1	23.3	14.4	23.0
1 j	>0		6.6	10.5	6.2	12.0

few occupied states of ^{208}Pb with other calculated and also observed values a reasonable agreement is found. For example, the single particle energy for 1 i state is 9.5 MeV which is in agreement with the experimental value of 9.0 MeV [10] for $1i_{13/2}$ state. The other corresponding calculated values are 8.5, 8.8, and 10.5 MeV quoted in Ref. [10-12] respectively. Table 1 also provides the comparison of the separation energies of the particles in deeply bound states. The energies calculated with the modified Skyrme interactions [12] are much too low for both nuclei ^{208}Pb and $^{298}_{114}X_{184}$ whereas Meldner's values for $^{300}_{114}X_{186}$ are larger than what are obtained from the velocity-dependent potential in these calculations. However, there is a good agreement for the first three states below the Fermi surface and a reasonable agreement with the next two or three states of these

calculations. Comparing the single-particle energy of the last occupied state, 1j in $_{114}^{298}\text{X}$ of our calculations, with those of Rost [11], Vautherin and Brink [12], and Dubna [13] for $1 j_{15/2}$ state which are 9.0, 9.0, and 10.6 MeV respectively, there seems to be a good agreement. There seems to be a partial magic number at the neutron number 170 from the level diagram of Mosel and Greiner [14]. The single-particle energies

for all states of neutrons in $_{114}^{284}\text{X}_{170}$ have also been presented.

From crude estimation based on the single-particle energies of last bond particles the superheavy nucleus $_{114}^{284}\text{X}_{110}$ seems to be stable against α-decay (or with long half-life time) which is consistent with Meldner's $_{114}^{284}\text{X}_{110}$. Other calculations also support the long half-life time except that of Brink [12] which has very short life-time for α-decay ($\sim 10^{-14}$ years).

[1] M. A. K. Lodhi, Phys. Rev. **182**, 1061 [1969] and references therein.
[2] W. E. Frahn and R. H. Lemmer,, Nuovo Cim. **5**, 1564 [1957] ; **6**, 664 [1957].
[3] A. M. Green, Phys. Letters **1**, 136 [1962] ; **3**, 60 [1962] ; Nucl. Phys. **33**, 218 [1962].
[4] M. Razavy et al., Phys. Rev. **125**, 269 [1962].
[5] A. Scotti and D. Y. Wong,, Phys. Rev. **138**, B 145 [1965].
[6] P. Roeper, Z. Phys. **195**, 316 [1966].
[7] H. Meldner, Phys. Rev. **178**, 1815 [1969].

[8] H. Meldner and G. Suessmann, Phys. Letters **6**, 353 [1963] ; Z. Naturforsch. **20 a**, 1217 [1965].
[9] J. Vogeler, Nucl. Phys. A **133**, 289 [1969].
[10] Noted in A. Bohr and B. R. Mottelson, Nuclear Structure, Vol. 1, W. A. Benjamin, Inc., New York 1969, p. 325.
[11] E. Rost, Phys. Letters **26 B**, 184 [1968].
[12] D. Vautherin and D. M. Brink, ,Phys. Letters **32 B**, 149 [1970].
[13] A. A. Sobiczewski, F. A. Gareev, ,and B. N. Kalinkin, Phys. Letters **22**, 500 [1966].
[14] U. Mosel and W. Greiner, Z. Physik **222**, 261 [1969].

Thermoluminescence of Deformed NaCl:Tl

R. V. Joshi and T. R. Joshi

Physics Department, M.S. University of Baroda, Baroda, India

Glow curves were recorded for annealed and quenched NaCl:Tl samples, compressed to tablets, after ultraviolet irradiation at room temperature. A marked difference in the shape of the glow curve for the first and second heating run has been observed. It is suggested that vacancy clusters and dislocation dipoles produced during deformation influence the thermoluminescence process of the deformed specimen.

The effect of quenching from different temperatures on the thermoluminescent behaviour of NaCl:Tl has been reported earlier [1]. It has been observed that, unlike other heat treated specimens, only the specimens annealed and quenched from a temperature close to the melting point exhibit a single, well developed peak at 390 °K. The purpose of this paper is to examine the effect of deformation on the thermoluminescence of thermally pretreated NaCl:Tl specimens. Specimens in the form of powder were prepared by crystallization from solution with varying Tl concentration. Spectroscopically pure sodium chloride supplied by Johnson, Matthey & Co., was used as host material. The powder specimens so obtainend were annealed and quenched from different temperatures and subsequently compressed to tablets in a stainless steel press. More or less similar results were obtained for specimens with different Tl content subjected to the above pretreatment. The results obtained in the case of the specimen with 0.03 mole percent Tl, quenched from 750 °C and then pressed to a tablet, shall be discussed. Thermal glow curves were recorded as described previously [2]
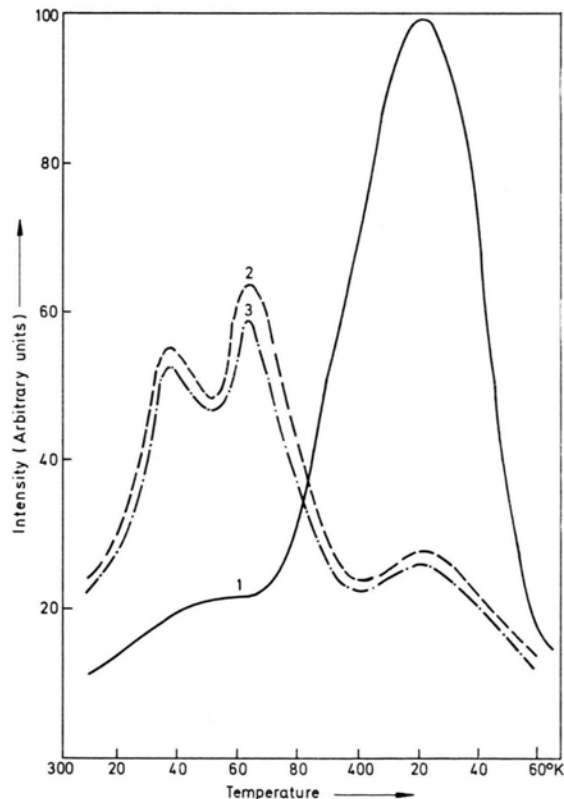
Fig. 1. Thermal glow curves for NaCl:Tl specimen quenched and then compressed to tablet. Curves 1, 2 and 3 represent the first, second and third thermal cycle respectively.

after warming the specimen at the rate of 10°/min. Figure 1, curve 1, which corresponds to the first thermal cycle, exhibits a pronounced glow peak at 420 °K

and a subsidiary peak around 340 °K. In the second heating run (curve 2) the 420 °K peak is considerably suppressed and two well defined peaks around 340 and 360 °K appear. The peak positions on the temperature scale were found to remain unchanged in the subsequent heating runs (curve 3).

It is now generally accepted that the plastic deformation of alkali halide crystals gives rise to dislocation debris in the form of vacancy clusters and dislocation dipoles [3-5]. It is therefore presumed that the centre responsible for 420 °K glow peak is a complex formed by the association of a Tl ion with a single vacancy or an aggregate of vacancies, the complex being situated in the dislocation region. At the end of the first heating run, when the specimen is heated to around 500 °K, a change in the distribution of the dislocations would take place to lower the strain energy of the microcrystals. Such a redistribution may involve both annihilation of dislocation dipoles and their alignment into low angle boundaries. To brinig about the rearrangement, both forms of motion (climb and slip) of edge dislocations are necessary. Since the dislocation climb depends on the movement of vacancies (an activated process), the rate of rearrangement increases rapidly with temperature. Thus by heating the specimen to around 500 °K, the dislocation content of the specimen will be reduced which in turn destroys the 420 °K centres.

The transformation of the 420 °K peak to 340 and 360 °K peaks, obvious in the second thermal cycle, suggests some kind of generic relationship between them. In other words some of the Tl^+ ions and the vacancy components of the 420 °K centres are used up in the formation of 340 and 360 °K centres. This is in accord with the nature of the centre proposed earlier [6] for the 340 °K glow peak in NaCl:Tl.

[1] R. V. JOSHI and T. R. JOSHI, Japan J. Appl. Phys. **10**, 1291 [1971].
[2] R. V. JOSHI, Proc. Phys. Soc. London **79**, 497 [1962].
[3] R. W. DAVIDGE and P. L. PRATT, Phys. Stat. Sol. **3**, 665 [1963].
[4] W. A. SIBLEY, Phys. Rev. **133**, 1176 [1964].
[5] R. CHANG, Phys. Rev. A **138**, 839 [1965].
[6] R. V. JOSHI and T. R. JOSHI, J. Luminescence **3**, 389 [1971].

BERICHTIGUNGEN

Zu M. DAKKOURI und H. OBERHAMMER, Molekülstrukturbestimmung von Trimethylazidosilan mittels der Elektronenbeugung an Gasen, Z. Naturforsch. **27 a**, 1331 [1972].

Seite 1335, rechte Spalte: In der dort abgebildeten Strukturformel muß es statt H_8 richtig H_3SiN_3 heißen. — Auf S. 1334, rechte Spalte, 14. Zeile von oben, ist der Satz „Auch während man für den ..." bis zum Schluß zu streichen.

H. JÄGER, Zur Entstehung primärer Gasentladungszonen bei elektrischen Drahtexplosionen, Z. Naturforsch. **27 a**, 1586 [1972].

Wegen zu späten Eintreffens der Korrektur konnten u. a. folgende Druckfehlerberichtigungen, Abänderungen bzw. Ergänzungen nicht mehr berücksichtigt werden:

S. 1587 r.,   9. Zeile: ... Drehspiegelanordnung mit Zwischenabbildung ...;
                30. Zeile: ... Impulse lösen nacheinander ...;

S. 1588 l.,   38. Zeile: ... danach scheinbar über einem ...;

S. 1590 r.,   letzte Zeile: ... der am Kondensator (im Sinne der reinen Kapazität zu verstehen) ...;

S. 1594 l.,   20. Zeile: $D < 5$ cm und Drahtdurchmesser $d \approx 0,05$ mm an dem der „offenen" Seite ...;
                24. Zeile: ... $E_r > 5 \cdot 10^5$ V/cm.

Zu Abb. 8:   — —, Nickeldraht.